

## On the connected-charges Thomson problem

Anže Slosar<sup>1</sup> and Rudolf Podgornik<sup>1,2,3</sup><sup>1</sup> Dept. of Physics, Faculty of Mathematics and Physics,  
University of Ljubljana, SI-1000 Ljubljana, Slovenia<sup>2</sup> University of California at Santa Barbara,

Kavli Institute of Theoretical Physics, Santa Barbara, CA 93106 USA

<sup>3</sup> Dept. of Theoretical Physics, J. Stefan Institute, SI-1000 Ljubljana, Slovenia

PACS. 82.70.Dd – Colloids.

PACS. 82.35.Rs – Polyelectrolytes.

PACS. 82.45.Gj – Electrolytes.

Abstract. – We investigate the modifications brought about by the linear connectivity among charges in the classical Thomson problem. Instead of packing with local hexagonal order interspersed with topological defects, we find charge distributions with helical symmetry wound around the surface of the sphere. This finding should have repercussions in the viral packing and macroion adsorption theories.

Introduction. – Electrostatics can be very unintuitive and can lead to quite unexpected features in a variety of physical, chemical and biological contexts [1]. The problem of packing charges on a sphere, generally referred to as the Thomson problem [2], has recently received a lot of attention and has been analysed via detailed direct numerical evaluation [3] as well as via approximate analytical theories [4]. What is clear is that for large enough number of charges the smallest electrostatic energy configurations have packing with local hexagonal order interspersed with topological defects [4]. A possible question here is: what happens if one linearly connects the charges and thus considers a linearly connected Thomson problem.

The linearly connected Thomson problem should be directly relevant for packing or adsorption of polyelectrolytes, i.e. charged polymers, on or to spherical surfaces. Adsorption of polyelectrolytes to spheres has been extensively simulated in the context of polyelectrolyte - macroion interactions in colloid physics [5]. Various configurations of adsorbed polyelectrolytes are seen, depending on the interaction parameters and the stiffness of the chain. Though they all correspond in one sense or another to a free energy minimisation as in the case of histone - DNA interactions [6], the phase space is simply too big in order to attempt some kind of systematic classification of shapes of the adsorbed polyelectrolyte chains. An "inverted" problem to the one just described is represented by the investigations of the nature of packing of DNA inside small bacteriophage capsids that has recently received a lot of attention since the nature of packing of DNA inside the capsid determines the ejection force that can be measured directly [7]. The only general and consistent conclusion stemming from these studies seems to be that DNA close to the capsid wall is more ordered than deep within the capsid. Recent cryomicroscopy on epsilon15 bacteriophage [8] gives ample experimental support for this type of order gradient within the viral capsid. At small packing fractions, where most or indeed all of DNA is expelled towards the inner surface of the capsid, the packing problem is directly related to the linearly connected Thomson problem.

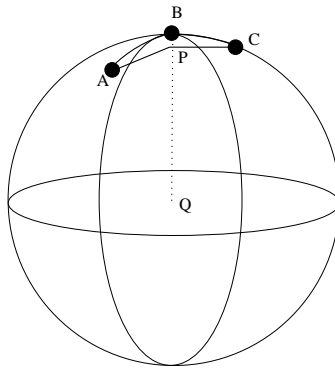


Fig. 1 – This Figure illustrates the geometry used in this paper. Three charges labelled  $A$ ,  $B$  and  $C$  lie on a surface of the sphere, whose centre is at  $Q$ . Point  $P$  is such that  $\overline{AP}$  and  $\overline{PC}$  are perpendicular to the line  $\overline{QB}$ . The angles  $\alpha_i$  used in this work correspond to  $\pi - \langle APC \rangle$ .

In order to shed some light onto packing of connected objects into confined spaces with spherical topology, we performed zero-temperature numerical investigations of the connected-charges Thomson effect. Apart from the fundamental significance of this problem [2] it could also be seen as a model of polyelectrolyte packing either on the outside or the inside of a sphere in the cases where the entropy of the chain can be neglected.

Model. – Our model system is composed of  $N + 1$  elementary charges connected by  $N$  rigid bonds of length  $\ell$  on a unit 3D sphere. Each rod subtends an angle  $\phi = 2 \sin^{-1}(\ell/2)$  with the centre of the sphere. The position of the charges are given by  $N + 1$  vectors  $\mathbf{x}_i$  ( $i = 1 \dots N + 1$ ), satisfying  $|\mathbf{x}_i| = 1$  and  $|\mathbf{x}_i - \mathbf{x}_{i-1}| = \ell$ . These constraints reduce the number of degrees of freedom to  $N + 2$ . Imposing rotational invariance further restricts the system to just  $N - 1$  degrees of freedom. The total length of the chain is  $L = N\phi$ . The Coulomb energy of this system is given by

$$E(L) = \sum_{i,j>i}^N \frac{1}{|\mathbf{x}_i - \mathbf{x}_j|} \quad (1)$$

It is useful for comparison to divide this value by the minimum energy the chain would have if it was not constrained to lie on a sphere. In that case, the minimum energy configuration would be a completely straight chain, whose energy is given by

$$E_0(L) = \sum_{i,j>i}^N \frac{1}{(j-i)\ell} = \frac{1}{\ell} (\Psi(N+1) + N(\gamma - 1)), \quad (2)$$

where  $\Psi$  is the standard digamma function and  $\gamma$  is the Euler's constant.

In the limit of large  $N$ , the minimal energy of an unconstrained Coulomb chain reduces to

$$E_0(L) \sim \frac{1}{\ell} N \log N \quad (3)$$

This has a fairly obvious explanation: for a long enough chain, most of the potential energy comes from the nearest neighbour interactions and therefore scales as  $N$ , while the Coulomb interactions between more remote charges contribute only logarithmically in  $N$ . This result is a signature of a completely extended Coulomb chain.

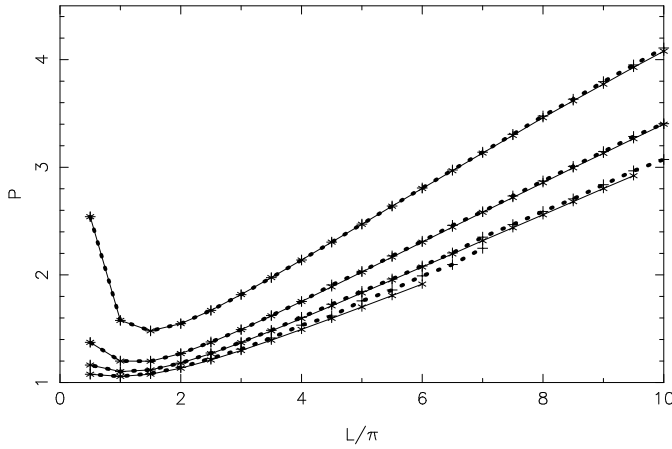


Fig. 2 – This figure shows the reduced potential energy as a function of the total chain length  $L$  for the four cases considered here:  $\phi = \pi/4$  (top),  $\pi/10$ ,  $\pi/20$ ,  $\pi/40$  (bottom). Solid line corresponds to the annealing in terms of  $\alpha_i$ , while the dotted thick line corresponds to annealing in terms of  $\beta_i$ . For large values of  $N$ , the computations become prohibitively expensive.

We define the reduced potential energy by

$$P(L) = \frac{E(L)}{E_0(L)}, \quad (4)$$

which measures the ratio between the Coulomb self-energy of a constrained and completely extended chain.

A natural description of this system is by  $N - 1$  angles  $\gamma_i$  subtended between rigid rods linking  $i - 1$ th,  $i$ th and  $i + 1$ th charge, i.e.  $\cos \gamma_i = (\mathbf{x}_i - \mathbf{x}_{i-1}) \cdot (\mathbf{x}_{i+1} - \mathbf{x}_i)$ . However, by projecting the mid-point down to the plane perpendicular to  $\mathbf{x}_i$  and going through  $\mathbf{x}_{i-1}$  and  $\mathbf{x}_{i+1}$  one arrives to a mathematically more convenient description in terms of the angles  $\alpha_i$ . We will define  $N - 1$  angles  $\alpha_i$  as

$$\cos \alpha_i = (\cos \phi \mathbf{x}_i - \mathbf{x}_{i-1}) \cdot (\mathbf{x}_{i+1} - \cos \phi \mathbf{x}_i). \quad (5)$$

The geometry of this choice of variables is illustrated on Figure 1.

Using straightforward geometry one can show that

$$\mathbf{x}_{i+1} = \cos \phi \mathbf{x}_i + \mathbf{f}_i \cos \alpha_i + \mathbf{p}_i \sin \alpha_i, \quad (6)$$

with

$$\mathbf{f}_i = \mathbf{x}_i \cos \phi - \mathbf{x}_{i-1} \quad (7)$$

and

$$\mathbf{p}_i = \mathbf{x}_i \times \mathbf{f}_i \quad (8)$$

By construction  $\mathbf{x}_{i+1}$  lies on a sphere if both  $\mathbf{x}_{i-1}$  and  $\mathbf{x}_i$  lie on a sphere. An  $\alpha_i = 0$  configuration corresponds to a linear, completely extended chain, while  $\alpha_i = \text{const.} \neq 0$  configuration results in charges being distributed along an arc on a spherical surface.

We will also use  $N - 1$  coefficients  $\beta_i$  that can be derived simply from a polynomial expansion of  $\alpha_i$  around the midpoint of the chain and are defined by

$$\alpha_i = \sum_{j=1 \dots N-1} \beta_j \left( \frac{i - N/2}{N/2} \right)^{j-1}. \quad (9)$$

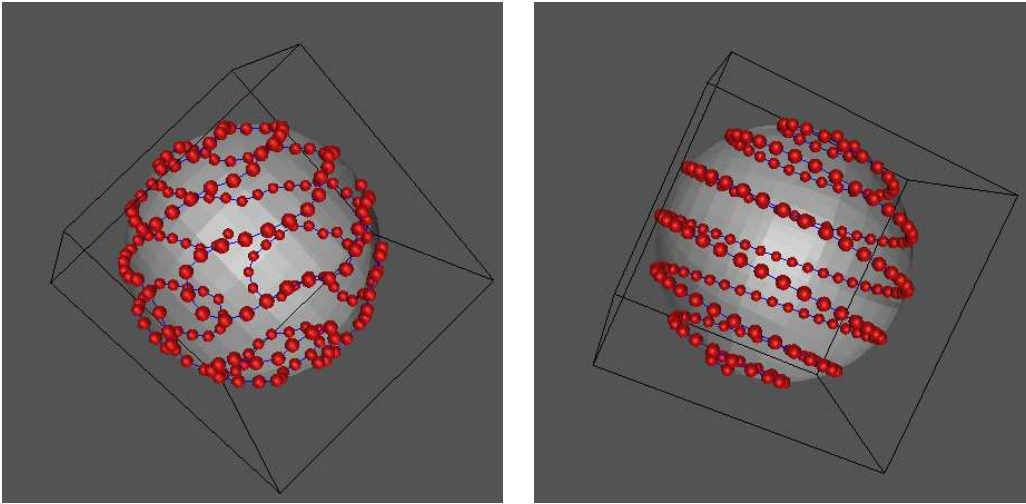


Fig. 3 – Typical minimum energy configurations for charges on a unit sphere. The l.h.s. corresponds to a typical solutions obtained with  $\alpha_i$  minimisation, while the r.h.s. is one obtained by  $\beta_i$  minimisation. Both are very similar (within better than 0.1%) in terms of the actual energy.

Description of the chain by  $\beta_i$  or  $\alpha_i$  is only a matter of convenience.

Saff and Kuijlaars [10] have shown that the "general spiral set" can be used to generate uniformly distributed points on a sphere. Their formalism can not however be directly applied to our problem, since the fixed links constrain the system further. Though we are not concerned explicitly with uniform distributions of points on a sphere, one can, nevertheless, reasonably expect that the minimal solution for the Thomson problem in the constrained case will exhibit helical behaviour. This is a hypothesis that we will try to investigate.

In order to set the terms of discussion, we recall the equation of a helix on a cylinder as given by  $z = ct$  and  $\phi = t$ . This can be generalised to a helix on a surface of a sphere by either identifying  $z$  with  $\cos \theta$  or  $\theta$ . We will denote the first case as embedded helix:

$$\begin{aligned}\theta &= \cos^{-1}(ct) \\ \phi &= t\end{aligned}\tag{10}$$

and the second one as spherical helix:

$$\begin{aligned}\theta &= ct \\ \phi &= t,\end{aligned}\tag{11}$$

where  $\theta$  and  $\phi$  are the ordinary spherical coordinates.

Results. – We have programmed software that finds the minimum energy configuration using two methods, working in either  $\alpha_i$  space or  $\beta_i$  space.

In the first case we anneal by angles  $\alpha_i$  using a version of genetic algorithm used in [9] for a classical Thomson problem. We start with a population of  $P$  "parents". We create  $P(P-1)/2$  "off-springs" by taking first  $N/2$   $\alpha_i$  values from the first parent and the remaining  $\alpha_j$ s from the second parent for all possible combinations of parents. We then use a simple numerical minimiser (downhill simplex) to find the local potential energy minimum corresponding to each parent. The best  $P$  solutions are kept and the process is repeated until a satisfactory convergence is reached. We typically work with 12 initial parents and 8 generations.

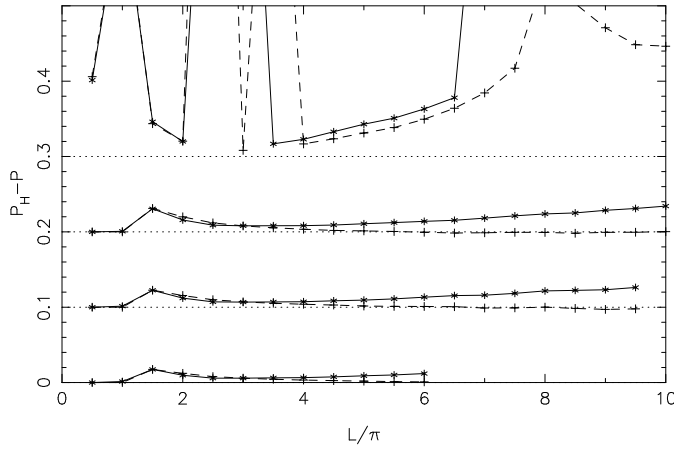


Fig. 4 – This figure shows the difference in reduced potential energy  $P$  between solutions found by full numerical minimisation and those found by constraining charges to lie on either embedded helix (solid) or spherical helix (dashed). Lines were offset vertically by  $i \times 0.1$  and correspond the four cases considered here:  $\phi = \pi/4$  (top),  $\pi/10$ ,  $\pi/20$ ,  $\pi/40$  (bottom). The dotted lines represent the zero difference value. For large values of  $N$ , the computations become prohibitively expensive.

In the second case we find the best solution by minimising the energy expressed in terms of parameters  $\beta_i$ . Genetic algorithm is not useful here as each  $\beta_i$  affects the entire chain and so good local features cannot be preserved. However, it is an extremely good space for optimisation and thus finds a good solution very quickly. After trying several options we have settled with an annealing algorithm that is a series of linear minimisers in randomly chosen parameters where the solution is assumed to be bracketed around the last optimal point and the width of the bracket is decaying exponentially until a desired convergence is reached. We typically try  $\sim 200$  different starting positions and then choose the best.

Finally, we have also minimised the energy of the system, whose charges are additionally constrained to lie on either embedded or spherical helix. Since this is a one-parameter model, the straight numerical minimiser performs satisfactorily. The purpose of this exercise was to check how well the true minimal configuration can be approximated by either helix.

We have run the minimiser with four values of  $\phi$ :  $\pi/4$ ,  $\pi/10$ ,  $\pi/20$  and  $\pi/40$  and for values of  $L$  ranging between  $\pi/2$  and  $10\pi$ .

In Figure 2 we plot  $P(L)$  as a function of the total chain length. It is immediately clear that both annealing procedures lead to stable solutions that are very similar in terms of energies for large enough values of the length of the chain. The well discernible minimum in the  $P(L)$  is easy to understand as follows: the energy  $E_0(L)$  is dominated by the nearest-neighbour contribution to the overall potential. The penalty paid by constraining the chain to lie on a sphere comes primarily from the “bending of the chain”. However, when  $L \gtrsim \pi$ , the  $E(L)$  receives another contribution from interaction between charges that lie far apart on the chain but a forced to lie close in physical coordinates due to wrapping of the chain around the sphere. Therefore, one can expect a minimum in  $P$  at around  $L/\pi \sim 1$  and this is exactly what we observe. However, we note that for a long enough chain, the reduced potential energy begins to scale nearly linearly with the chain length.

Naively, one would expect that the energy of the electrons on the chain wrapped on a sphere would scale with  $N$  roughly as  $N^2$  and so the reduced potential energy  $P$  should scale as  $N/\log N$  for large  $N$ . Our data do not extend high enough in  $N$  to discriminate unequivocally between

linear and  $N/\log N$  scaling, though the latter indeed provides a marginally better fit to the data. Interestingly enough, this is the true even for cases when values of  $E_0$  have not yet reached the  $N \log N$  scaling.

We also note, that although very similar in energy, the solutions found by the  $\beta_i$  annealing procedure are always helical, while the solutions in terms of the  $\alpha_i$  annealing procedure are, for large enough  $N$ , configurations that are locally (on a sphere, not along the chain) helical but are irregular on large scales. This is illustrated in the Fig. 3. What we are likely seeing is a plethora of metastable configurations with nearly minimal energy, similar to those found for a classical Thomson problem. This is supported by two observations: firstly, making minimiser convergence criteria stronger does not improve these solutions, implying that they are indeed meta-stable and secondly, all final generation solutions in the genetic algorithm have very similar energies (to within a few pro-miles) and are different on runs with different random seeds, implying that the family of those solutions is quite large. These nearly minimal configurations are never found by the  $\beta_i$  annealing as this would require a coherent tuning of several  $\beta_i$  coefficients to achieve a preferred local behaviour. The existence of a large number of these nearly minimal configurations also implies that unless a specific mechanism is in place, the chain is very likely to land in a complex nearly-perfect meta-stable state rather than the helical structure with long-scale ordering.

Next let us discuss the solutions which come from constraining the charges to lie on either of the two helices defined in Eqs. (11) and (10). Results are plotted in the Figure 4. It can be seen that for chains with  $\phi \lesssim \pi$ , the spherical helix is an increasingly better approximation to the true minimum for large enough  $L$ . It thus appears that we are able to construct explicitly those configurations that are close to optimal. This confirms our expectations based on the "generalised spiral set" of Saff and Kuijlaars [10] that solutions with helical symmetry should describe minimal energy states for the connected-charges Thomson problem.

Conclusions. – In this paper we have analysed the connected-charges Thomson problem by brute-force numerical minimisation of the potential energy. The problem is completely specified by two parameters:  $L$ , the total length of the chain, and  $\phi = L/N$ , that defines the inter-charge separation. Note that the links between the charges are inextensible.

We have found that for all cases considered, the reduced potential energy has a minimum at  $L/\pi \sim 1$  and scales as  $N$  or  $N \log N$  (the range of  $N$ s investigated does not extend to large enough  $N$  so that one could differentiate between the two scaling forms). This implies furthermore that the potential energy of the chain scales as  $N^2$  for large  $N$  as expected from standard arguments. However, the relation is true even for  $N$  that are so low that  $E_0(N)$  has not reached the  $N \log N$  scaling yet.

We have heuristically attempted to model the minimum energy configuration with a helix on a sphere. We have found that the cylindrical helix projected onto a sphere by a simple transformation  $z \rightarrow \theta$ , thus creating a spherical helix, leads to charge configurations that seem to be very close to the numerically obtained minimum for  $L \gtrsim \pi$  and  $\phi \ll 1$ . The solution is likely to continue in such manner until the distance between points that are far apart along the helix but close in real space becomes important. This would result in a frustrated helix that might hide new and exciting phenomenology. Unfortunately, the presently available computers do not reach the computational power necessary to answer this question, at least not with the methods provided in this paper.

What is the physical relevance of our results? Adsorption of flexible polyelectrolytes onto spherical macroions (colloidal interactions) and configurations of polyelectrolytes within spherical cavities (viral packing) both belong to the type of problems which have been analysed in this paper on their bare bones level. Though in general the configurations of real polyelectrolyte chains

depend on many parameters and are difficult to classify [11], our analysis provides an asymptotic limiting configuration that should be discernible in the case where adsorption interaction onto a spherical macroion is strong enough, or the repulsive interactions along the chain in a spherical cavity are sufficiently long-ranged. An especially beautiful illustration of our theory is provided by recent elucidation of the DNA packing inside the epsilon15 capsid [8] that shows tight helical winding on the outer boundary and the progressive loosening of the orientational order as one moves away from the boundary towards the interior of the capsid.

Acknowledgement. – RP and AS acknowledge the financial support of the Agency for Research and Development of Slovenia under the grants P1-0055(C) and Z1-6657 respectively. This research was also supported in part by the National Science Foundation under Grant No. PHY99-07949.

#### REFERENCES

- [1] Y. Levin, *Physica A*, 352 (2005) 43. H. Boroudjerdi, Y.W. Kim, A. Naji, et al. *Phys Rep* 416 (2005) 129.
- [2] Y. Levin and J.J. Arenzon, *Europhys. Lett*, 63 (2003) 415.
- [3] E.L. Altschuler et al., *Phys. Rev. Lett.*, 78 (1997) 2681.
- [4] M. Bowick et al., *Phys. Rev. Lett.*, 89 (2002) 185502.
- [5] J. Dzubiella, A. G. Moreira and P. Pincus, *Macromol* 36 (2003) 1741. P. Chodanowski and S. Stoll, *Macromol* 34 (2001) 2320. A. Akhinchina and P. Linse, *Macromol* 35 (2002) 5183. A. Akhinchina and P. Linse, *J. Phys. Chem.* 107 (2003) 8011.
- [6] H. Boroudjerdi and R.R. Netz, *Europhys Lett* 71 (2005)1022.
- [7] J. Arsuaga et al., *Biophys. Chem.* 101 (2002) 475. J. Kindt et al. *Proc. Natl. Acad. Sci.* 98 (2001) 13671. A.J. Spakowitz and Z.-G. Wang, *Biophys. J. BioFAST* (2005) biophysj.104.052738. W.S. Klug, M.T. Feldmann, M. Ortiz, *Comput. Mech.* 35 (2005) 146.
- [8] W. Jiang et al. *Nature* 439 (2006) 612.
- [9] J.R. Morris, D.M. Deaven and K.M. Ho, *Phys. Rev. B* 53 (1996) R1740.
- [10] E. Saff and A. Kuijlaars, *Mathematical Intelligencer* 19 (1997) 5.
- [11] K.K. Kunze and R.R. Netz *Phys. Rev. E* 66 (2002) Art. No. 011918. K.K. Kunze and R.R. Netz, *Europhys Lett* 58 (2002) 299.